Exploring the dual dynamic synergy of transesterification and siloxane exchange in vitrimers

Sami Fadlallah, Filip van Lijsebetten, Tapas Debsharma, Vincent Scholiers, Florent Allais, Filip Du Prez

Exploring the Dual Dynamic Synergy of Transesterification and Siloxane Exchange in Vitrimers

Sami Fadlallah,[ab] Filip Van Lijsebetten,[a] Tapas Debsharma,[a] Vincent Scholiers,[a] Florent Allais,[b] Filip E. Du Prez*[a]*

[a] Polymer Chemistry Research group, Centre of Macromolecular Chemistry (CMaC), Department of Organic and Macromolecular Chemistry, Faculty of Sciences, Ghent University, Krijgslaan 281-S4, Ghent, 9000, Belgium.

[b] URD Agro-Biotechnologies Industrielles (ABI), CEBB, AgroParisTech, Pomacle, 51110, France.

KEYWORDS. Covalent adaptable networks, vitrimers, recyclable thermoset, dual dynamics.

ABSTRACT

Despite the benefits of dynamic polymer networks with multiple dynamic bonds, identifying compatible combinations of dynamic chemistries that work synergistically to achieve desirable properties remains a significant challenge. This work focuses on the potential of utilizing both siloxane and ester dynamic bonds in epoxy-acid cured vitrimers to finetune chemical exchange

reactions. We identified to what extent a common basic catalyst (TBD) can simultaneously activate siloxane and ester exchange in the corresponding epoxy-based vitrimers. Our results showed that TBD is not only able to facilitate network formation but also improved the dynamic behavior of the resulting networks dramatically, with an overall exchange rate that is faster than the sum of the individual exchange chemistries, as shown by stress-relaxation studies. It has been demonstrated that the siloxane and ester dynamic bonds work together in a synergistic way to facilitate topology rearrangement. The relative increase or decrease in mobility of neighboring chains, located around a specific dynamic bond within the polymer network, was investigated in detail by adjusting the concentration of dynamic bonds and catalyst. The herein reported strategy allows the production of dual dynamic polymer networks that exhibit much shorter relaxation times and thus improved (re)processability in comparison to vitrimers with one type of dynamic bond.

INTRODUCTION

Thermosets possess remarkable dimensional stability, stiffness, and chemical resistance.[1] However, due to their permanent covalent cross-links, they are not suitable for recycling or reshaping.[2] To overcome this limitation, researchers have been exploring reversible cross-linking strategies to introduce plasticity into thermosets, thus improving their recyclability.[3–7] Since 2011, vitrimers have emerged as a promising class of dynamic materials that enable chain mobility and plastic deformation through heat-driven chemical exchange of the constituting covalent cross-links.[8–10] Unlike other reversible networks, vitrimers can facilitate material flow by associating cross-links with reactive species, without undergoing complete dissociation of their dynamic bonds.[11,12] The rate-limiting step of this macroscopic process is primarily

determined by the rate of a chemical reaction, provided that the diffusion of network components is fast enough.[13]

Given the obvious link with chemical reaction kinetics, it is not surprising that catalysis has been an integral aspect of vitrimer research since its inception.[14–21] Since the seminal work of Leibler and co-workers on Zn-catalyzed transesterification in epoxy-acid cured vitrimers,[8] several dynamic covalent chemistries have been reported and are nicely summarized in numerous comprehensive reviews.[22–24] Despite the increasing number of chemical platforms, transesterification remains the most widely investigated vitrimer system because of its ease of use and similarity to a type of conventional thermoset formulations.[25–33]

While several strategies have been reported to control the dynamics of vitrimers, one intriguing method is to rethink the design of the macromolecular architecture to promote polymer chain diffusion and reactivity.[11,21] This can be achieved by altering the cross-link density or introducing network defects to impact the intrinsic elasticity of vitrimers, thereby improving their reprocessability.[34–38] Additionally, the availability of reactive species plays a crucial role in the rate of macroscopic material flow.[12,39] To this end, depending on the specific design choices, three general strategies can be distinguished: the targeted reduction in dynamic bonds to control the density of reversible cross-links (Scheme 1a),[40–42] the dilution of dynamic units, which involves the use of macromolecular non-reactive segments (Scheme 1b),[43,44] and the synergistic use of multiple dynamic motifs which has gained prominence (Scheme 1c).[39,45–53] This latter strategy employs a combination of different reactive chemistries to design materials with tailor-made viscoelastic profiles that can match user-defined specifications.[54–56]

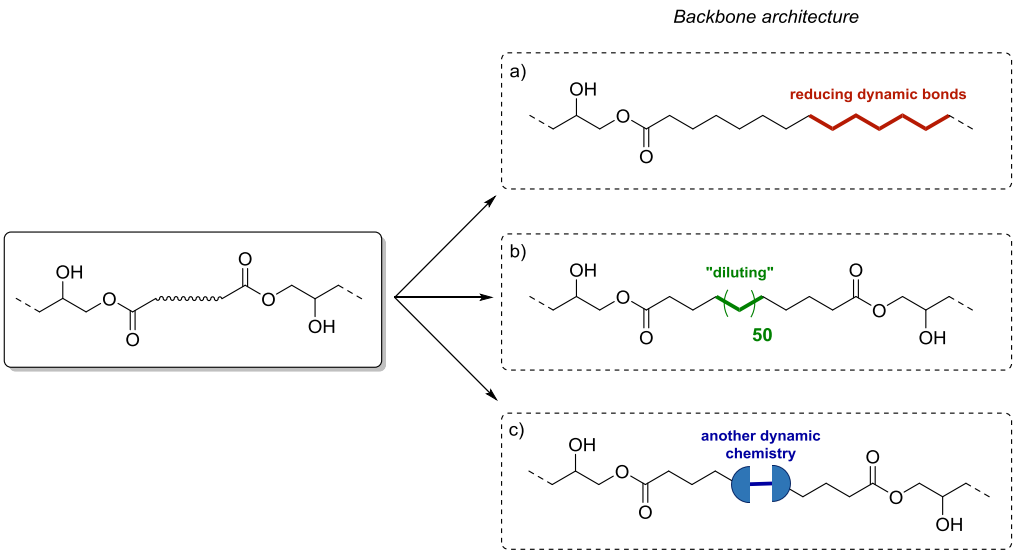

Scheme 1. The primary techniques utilized to manage the dynamics of vitrimers, exemplified for an epoxy-acid cured matrix.

Understanding and manipulating the criteria for true orthogonality or synergy between different dynamic cross-linkers remains an important challenge in the field.[57] At a shorter timescale, a dynamic bond may act as a "permanent linker" and put constraints on polymer chain diffusion, while at a longer timescale it may induce movement of polymer chains. The tendency for movement of neighboring polymer chains on a dynamic bond will have an important effect on the average relaxation rate of the overall polymer network.

Intrigued by the possibilities in creative macromolecular design, we herein studied the synergy of two dynamic covalent chemistries within epoxy-based vitrimers (**Scheme 2a**). Specifically, transesterification and siloxane exchange were intentionally chosen because both associative mechanisms involve hydroxyl groups, and are able to interact with the same basic organo-catalyst (*e.g.*, triazabicyclodecene or TBD, Scheme 2b). Moreover, we recently reported that siloxane bonds exhibit quite fast exchange properties when combined with TBD and hydroxyl groups.[20] Finally, the inherent stability and resistance of siloxane bonds to

degradation and hydrolysis make siloxane-based materials highly desirable for a multitude of industrial applications, including silicone elastomers and biomedical materials, for which longevity and reliability are critical.[58]

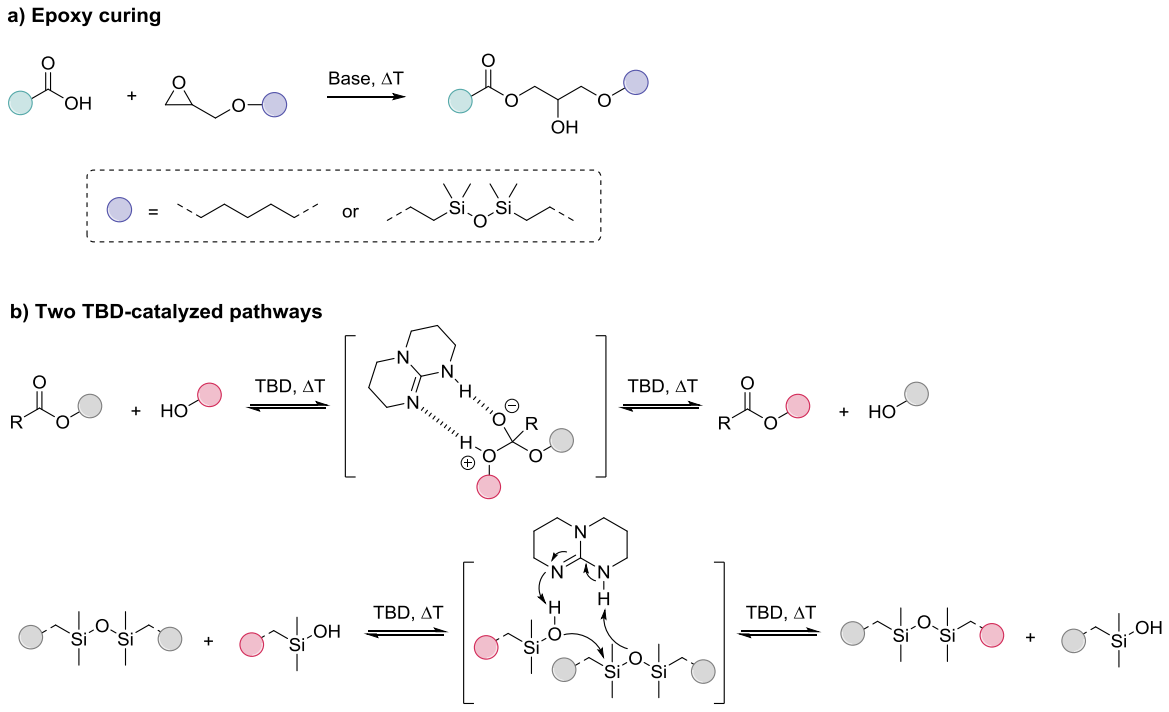

Scheme 2. Design strategy for dual exchange vitrimers reported herein. a) Epoxy-acid curing using different functional monomers, and b) two synergetic associative dynamic covalent chemistries based on ester and siloxane exchange, catalyzed by the same basic catalyst TBD.

Adjusting the stoichiometry of the reactants or the catalyst loading may have an effect on both chemistries, establishing their inherent synergy. To demonstrate this hypothesis, vitrimers containing both esters and siloxane groups were synthesized using commercially available compounds. The dynamic properties of these polymer networks, containing dual dynamic groups, were analyzed using rheological experiments, and compared to reference materials involving transesterification or siloxane exchange, individually. Additionally, different models were utilized to differentiate and identify each reactive segment and characterize the exponential decay of the stress relaxation behavior of the materials.[59] Importantly, in contrast to previously

reported crosslinked materials containing multiple dynamic groups, this approach enabled us to reveal the origin of the rapid processability of the siloxane-ester materials and allow for tuning material properties to cover a larger application scope. To demonstrate the versatility of the proposed system, additional adjustments were made to the composition and amount of the constituting components. These optimizations were aimed at achieving an optimal balance between dynamicity and creep resistance.

EXPERIMENTAL

Chemicals. 1,5,7-Triazabicyclo[4.4.0]dec-5-ene (98%) (TBD), hexanoic acid (>99.5%) (HA) and 1,2,7,8-diepoxyoctane (DiEpoxOct) were purchased from Sigma Aldrich (Merck). 1,3-Di(3-glycidyloxypropyl)tetramethyldisiloxane (97%) (DiEPoxSilox) was purchased from Gelest, Inc. 4,4′-Methylenebis(*N*,*N*-diglycidylaniline) (TetraEpox) and 1,3-bis(aminomethyl)cyclohexane (BA) were purchased from TCI. Sebacic acid (98%) (SA) was purchased from Acros Organics.

Instrumentation. Fourier-transform infrared spectroscopy (FTIR) spectra were recorded on a Cary 630 FTIR Spectrometer by Agilent. Nuclear Magnetic Resonance (NMR) analyses were conducted on a Bruker Avance 300 (300 MHz). The NMR spectra were measured in $CDCl_3$, and chemical shifts (δ) are presented in parts per million (ppm), relative to $CDCl_3$ as the internal standard. Differential Scanning Calorimetry (DSC) was performed with a Mettler Toledo instrument 1/700. Typically, ~12 mg sample was placed in a sealed pan, flushed with nitrogen gas and passed through a heat-cool-heat cycle at 10 °C/min in a temperature range of -100 °C to 100 °C. Three heat/cool cycles were done for each sample, where the last two cycles were dedicated to analyzing the heat flow of the sample after being cooled in controlled conditions. The T_g values recorded herein are those obtained from the third cycle.

Thermogravimetric Analysis (TGA) was measured with a TGA Q500 (TA Instruments). Typically, ~2 mg of each sample was equilibrated at 50 °C for 30 min and was flushed with nitrogen gas. All the experiments were performed with a heating rate of 10 °C/min up to 600 °C. The reported values of $T_{d5\%}$ represent the temperature at which 5% of mass is lost. Isothermal TGA was measured with a TGA Q500 (TA Instruments). Typically, ~5 mg of each sample was equilibrated at 50 °C for 5 min and was flushed with nitrogen gas. For (siloxane-)ester and siloxane-based substances, the tests involved heating up to 160°C and 220°C (the temperature utilized during hot pressing), respectively. Subsequently, the temperature was maintained for 25 min for siloxane-ester, 40 min for ester, and 50 min for siloxane materials. Rheology experiments were performed on an Anton Paar MCR 302. The experiments were performed in parallel plate geometry using sample disks having a diameter of 8 mm and a thickness of about 2 mm. Stress-relaxation experiments were performed at different temperatures (200 to 150 °C, with intervals of -10 °C) using a constant shear strain of 1% and a constant force of 1 N under nitrogen. Each measuring step was preceded by a force normalization step of 1 N, while monitoring the gap between each plate. Creep experiments at different temperatures (30-120 °C, with intervals of +10 °C) were also performed using a constant force of 1 N. Additionally, in the first 300 s no shear stress was applied. Following this, a 2000 Pa shear stress was applied for 5000 s, without recovery. Creep measurements were preceded by a time sweep measurement at 90 °C and fixed frequency of 1 Hz for 1 h to remove possible thermal history.

Synthesis of polymer networks (typical procedure).

Siloxane-containing networks (Scheme 3). The hardener (BA, 1,3-bis(aminomethyl)cyclohexane) was added in a 20 mL cup, followed by TBD (5, 7.5, or 10 mol% with respect to DiEPoxSilox). The compounds were mixed using a speedmixer® (DAC 150.1

FVZ) for 2 min at 3500 rpm. In a second step, 0.9 eq. (based on BA) of DiEpoxSilox was added and mixed at 3500 rpm in the speedmixer® until a homogeneous phase was obtained (approximately 30 sec). Finally, the resulting sample was heated to 50 °C for 14 h, then 60 °C for 14 h, before being post-cured at 85 °C in a vacuum oven for 24 h. The manufacturing process employed 5 mol%, 7.5 mol%, and 10 mol% TBD, resulting in the samples being designated as Am-1, Am-2, and Am-3, respectively (Scheme 3). These are the only samples within this study that incorporate an amine (Am) hardener for their fabrication.

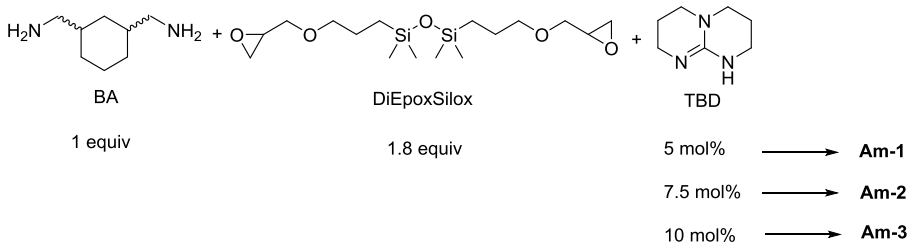

Scheme 3. Synthesis of siloxane-based networks (Am-1, Am-2 and Am-3).

Siloxane-ester networks (see Table 1 for ratios of each compound). The diepoxide molecule(s) (DiEpoxSilox or/and DiEpoxOct, Scheme 4) was (were) first placed in a 20 mL cup. Then, a certain amount of TBD catalyst was added to the cup, depending on the formulation being used. For all formulations of siloxane-ester networks reported in Table 1 (except TBD-5%), the same amount of catalyst was used, i.e., 68.83 mg of TBD catalyst. Only one sample (named as TBD-5% in Table 1), used 34.41 mg of TBD catalyst.

More precisely, the amount of catalyst used was chosen to correspond to 10 mol% catalyst (except for TBD-5%) with respect to sebacic acid (SA) (1 g) for the following formulations: TBD-10%, Sil-0%, Sil-25%, Sil-50%, and Sil-75% (Table 1). For acid content screening, the amount of TBD catalyst was kept constant at 68.83 mg to allow comparison, while the amount of acid content was varied. Specifically, the acid content was decreased from 1 g for

TBD-10% to 0.75 g for Ac-75%, then to 0.5 g for Ac-50%, and finally to 0.25 g for Ac-25% (Table 1).

The compounds were stirred in a speedmixer® (DAC 150.1 FVZ) for 8 min (4 x 2min) to form a clear solution and dissolve TBD, followed by TetraEpox. SA was then added to the prepared epoxide-TBD mixture and heated to 60 °C. The mixture was then left to stir vigorously for 14 h at 60 °C. Thereafter, the temperature was increased to 80 °C and stirring was continued until a clear, completely homogeneous mixture was obtained (approximately 2 h depending on the reactant ratios). The resulting product was left to cure for a period of 6 h, then placed in a vacuum oven at 110 °C for 16 h and then post-cured at 145 °C for 4 h. A series of samples were produced with different epoxide/SA ratios (summarized in Table 1).

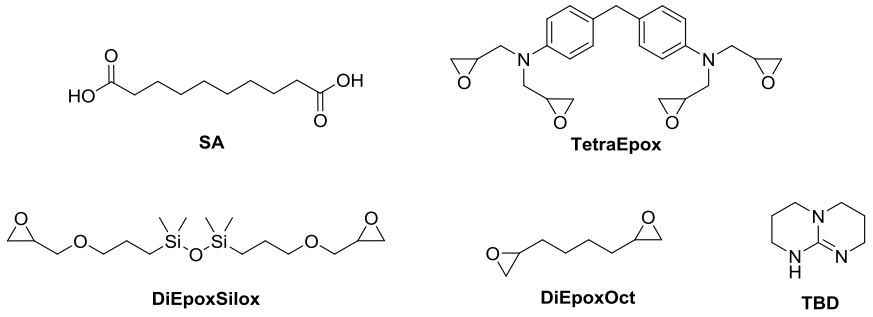

Scheme 4. Reactants and organo-catalyst used in the synthesis of siloxane-ester networks.

Table 1. Overview of compositions and physical properties of siloxane-ester networks.

Screening	Sample label	Eq. ac.(SA)/ Eq. epox.	Total Epoxide Content (mol%)			T_g (°C)[a]	$T_{d5\%}$ (°C)[b]	Swelling ratio (%)[c]	Soluble fraction (%)[c]
			Tetra Epox	DiEpox Sil	DiEpox Oct				
Catalyst loading	TBD-5%	1/1	25	75	0	-34	237	342 ± 2	15.8 ± 0.2
	TBD-10%	1/1	25	75	0	-31	233	204 ± 4	8.7 ± 0.3
Siloxane[d] content	Sil-0%	1/1	25	0	75	-5	280	168 ± 4	7.3 ± 0.9
	Sil-25%	1/1	25	18.75	56.25	-12	254	249 ± 2	17.3 ± 0.4
	Sil-50%	1/1	25	37.5	37.5	-20	241	229 ± 8	11.9 ± 0.3
	Sil-75%	1/1	25	56.25	18.75	-25	233	280 ± 22	16.5 ± 0.3
Acid content[e]	Ac-25%	0.25/1	25	75	0	-5	256	136 ± 5	1.9 ± 0.8
	Ac-50%	0.5/1	25	75	0	-18	240	154 ± 3	4.2 ± 0.4
	Ac-75%	0.75/1	25	75	0	-25	227	182 ± 7	6.2 ± 0.4

[a] Glass transition temperature determined by DSC, third heating step, temperature ramp 10 °C/min. [b] TGA degradation temperatures at which 5 % ($T_{d5\%}$) mass loss was observed under nitrogen. [b] Swelling ratio and soluble

fraction were calculated by gravimetry. [d] The percentages in the sample label represent the proportion of DiEpoxSil relative to the total amount of diepoxide molecules (DiEpoxSil and DiEpoxOct). The percentages in the sample label indicate a decrease in the amount of SA from 1 g to 0.75 g (Ac-75%), 0.5 g (Ac-50%), and 0.25 g (Ac-25%) respectively.

Material reprocessing (Figure S1, ESI)**.** The polymer samples were cut into 1-mm-sized pieces and placed in a two-part rectangular-shaped steel mold (30 mm × 15 mm) for compression molding. This assembly was placed for 2 min under a pressure of 1 metric ton in a hydraulic press (hot press) that is preheated to 160 °C in the case of siloxane-ester materials and 220 °C for siloxane networks. Then the pressure (by means of weight) was increased to 3 or 4 tons and held constant for an additional time. The total pressing time ranged from 20 to 45 minutes, depending on the material, with longer durations required for siloxane materials (45 min), followed by ester (35 min) materials, then siloxane-ester materials (20 min). After completion of the pressing, the mold was allowed to cool for 3-5 minutes before the sample was removed.

Swelling and soluble fraction analysis. The tests were performed on approximately 70-80 mg polymer samples at 25 °C in 6 mL THF. The swollen samples were removed after 3 days, wiped with a tissue, and swelling ratio was calculated as follows:

$\text{swelling ratio (\%)} = \frac{m_s - m_i}{\mathrm{m}_i}$, where m_s is the swollen mass and m_i is the initial mass.

In order to determine the soluble fraction, the materials were immersed in THF for a total of six days. To ensure accuracy of the measurement, the THF was replaced with a fresh batch (6 mL) after three days, which coincided with the time when the samples were taken to calculate the swelling degree. After 6 days, the solvent was removed, and the samples were dried under vacuum overnight at 50 °C. The soluble fraction was calculated as follows:

$\text{soluble fraction (\%)} = \frac{m_i - m_d}{\mathrm{m}_i}$, where m_d is the mass after drying and m_i is the initial mass.

RESULTS AND DISCUSSION

Since the physical properties and material flow tendency of vitrimers are determined by the rate of chemical exchange reactions, we sought to investigate methods for controlling this rate. Specifically, we examined the combination of siloxane and ester dynamic bonds within a single vitrimer material, which are both responsive to the same catalyst (TBD). Our initial hypothesis was that the rate of chemical exchange reactions could be modulated through the variation of both siloxane and ester dynamic bond concentrations, as well as that of TBD, within the vitrimer material. This, in turn, could result in notable alterations in the physical properties and material flow characteristics of the produced vitrimers. To achieve this purpose, we prepared three different series of networks, each focusing on a different aspect of the vitrimer: catalyst loading, siloxane content, and ester content. The vitrimer materials were prepared by mixing the diepoxide molecule(s) with TBD as the catalyst, TetraEpox as a cross-linker, and sebacic acid as shown in Scheme 4. These monomers were readily accessible, allowing for efficient synthesis and characterization of the dual dynamic networks. Moreover, TetraEpox was incorporated not only as a crosslinker to promote network formation but also to impart an internal catalytic function to the resulting structure. Indeed, the presence of tertiary nitrogen in crosslinkers, such as TetraEpox, has been shown to facilitate transesterification without the need for an external catalyst. For example, in a recent study, polyester vitrimers containing internal tertiary amine moieties demonstrated efficient bond exchange as a result of internal catalysis provided by tertiary amines, enhancing the recyclability and reshaping potential of vitrimers under mild conditions.[60]

After the initial curing process, the mixture underwent an additional post-curing treatment (145 °C, 4 h) to promote network equilibration through transesterification reactions. This method resulted in vitrimer materials suitable for investigating the rate of chemical exchange reactions

and their impact on physical properties and dynamic behavior. Two reference samples were also prepared: the first used the same procedure but substituted DiEpoxSilox with DiEpoxOct, resulting in an "only ester-based network". The second was composed solely of a siloxane-based network, as illustrated in Scheme 3, and Table S1 in the ESI. These reference systems enabled a comprehensive assessment of the contributions of siloxane and ester dynamic bonds to the properties of the vitrimer materials.

Monitoring network formation with FTIR

Fourier transform infrared spectroscopy (FTIR) was utilized to track the development of the network formation. The successful completion of the curing process was confirmed by observing the disappearance of the carboxylic acid stretching band of SA at 1684 cm^{-1}, and the appearance of an ester formation band at 1740 cm^{-1} resulting from the reaction between the carboxylic and epoxide moieties (Figure S2, ESI). This reaction resulted also in the formation of a hydroxyl band at 3435 cm^{-1}. Furthermore, the complete elimination of the characteristic epoxide peaks of TetraEpox (972-890 cm^{-1}) and DiEpoxSilox (905 cm^{-1}) is evident in Figure S3 (ESI).

To gain more insights into the effect of TBD, DiEpoxSilox and hexanoic acid were reacted with and without TBD separately, and the reaction mixtures were analyzed by ^{1}H NMR (Figure S9, ESI). No additional reaction between the epoxide and acid groups was detected in the absence of TBD. On the other hand, the presence of TBD led to the formation of new peaks in the region 3.5-5.5 ppm, suggesting an addition reaction and/or anionic ring-opening polymerization (ROP) of epoxide moieties.[31] TBD was found to catalyze the addition reaction between the epoxide and acid groups, resulting in the creation of a polyhydroxy ester network.

Additionally, as illustrated in Figure 1, the formation of ether bonds via anionic ROP between epoxide groups was identifiable through the observation of peak (4) at 1091 cm^{-1}. It is also evident that the presence of siloxane groups had no significant impact on polyaddition compared to ROP. Indeed, changing the ratios between DiEpoxSilox and DiEpoxOct mainly affected the Si-CH_3 (3) and Si-O-Si (5) bands, which decreased considerably in the case of Sil-25% (Figure 1) and were not observed for a purely ester-based network (Sil-0%, Figure S8, ESI). On the other hand, the amount of acid content had a significant impact on the network structure formed. For instance, in the case of Ac-25%, the lowest acid content compared to the epoxide content (0.25:1) led to a notable increase in the peak (4) at 1091 cm^{-1}, indicating that anionic ROP was the predominant mechanism, resulting in a predominantly polyether-based network. However, increasing the acid content to 50% and 75% (Ac-25% and Ac-75%, respectively) decreased the intensity of the peak that is correlated to polyether formation (Figure S5, ESI). In a similar epoxy-acid system, it was suggested that etherification does not occur until the addition reaction is complete.[31] This indicates that, in conditions of 1:1 stoichiometry, the ester formation is predominant. Although other reactions, such as Fischer esterification of free hydroxyl and acids, as well as transesterification of hydroxyl and ester bonds, could potentially occur,[31] FTIR analysis did not detect any evidence of their formation. Specifically, a new ester peak accompanied by the disappearance (or decrease) of the original ester peak was not observed.

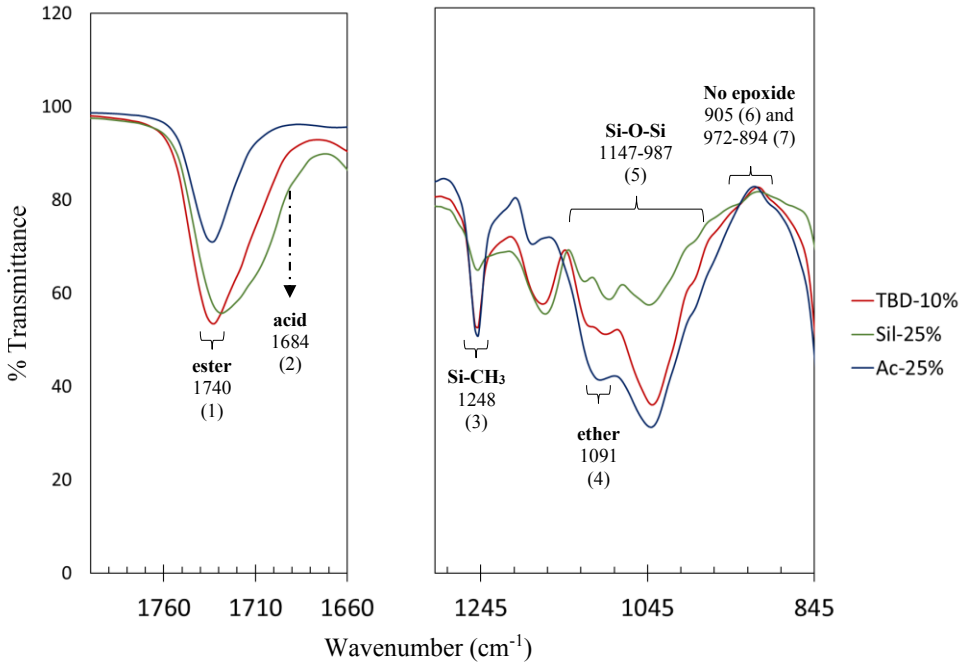

Figure 1. FTIR spectral curves of TBD-10%, Sil-25% and Ac-25%.

Thermal analysis of vitrimers

The impact of chemical composition on the thermal properties of the polymer networks was also studied. This was accomplished by analyzing the networks, reported in Table 1, using differential scanning calorimetry (DSC) and thermogravimetric analysis (TGA) (Figure 2 and Table 1). The results showed that decreasing the SA content resulted in an increase of the glass transition temperature (T_g) (Figure S12, ESI) and the temperatures corresponding to a 5% weight loss ($T_{d5\%}$) (Figure S16, ESI), which could be attributed to an increase in the proportion of the crosslinked polyether segments in the network. Conversely, increasing the amount of DiEpoxSil resulted in a decrease in T_g and $T_{d5\%}$ ranging from -5 to -31 °C (Figure S11, ESI) and 256 to 223 °C (Figure S15, ESI), respectively. In addition, the effect of the aliphatic chain length and the type of the epoxide precursor (DiEpoxSil vs. DiEpoxOct) on the thermal properties was also explored. A composition with a reduced fraction of DiEpoxSil, thereby increasing the fraction of

DiEpoxOct containing shorter carbon-carbon aliphatic chains, led to a more rigid network, evidenced by the rise in T_g (from -25 to -5 °C) and $T_{d5\%}$ (233 to 280 °C). It is worth noting that all samples analyzed in this study exhibited $T_{d5\%}$ values above 227 °C, far exceeding the temperatures required for both ester transesterification and siloxane exchange. Additionally, the thermal decomposition of the siloxane-ester networks can be distinguished by two stages: the initial dissociation of esters and the subsequent decomposition of siloxane bonds (Figure S15-S17, ESI). The isothermal TGA experiments showed that a mass loss of approximately 1-3% was recorded at 160°C after 20 min for (siloxane-)ester materials (Figure S19-S21, ESI).

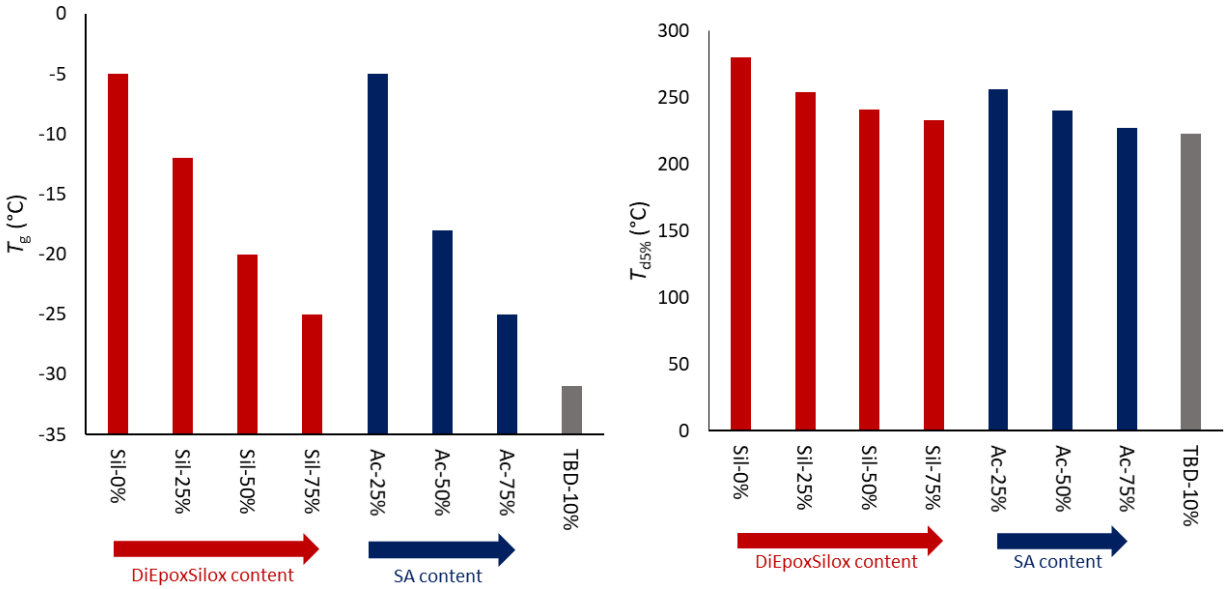

Figure 2. Evolution of T_g and $T_{d5\%}$ as a function of the DiEpoxSilox and SA content of the vitrimers.

Swelling and soluble fraction analysis

Table 1 summarizes the outcome of the swelling experiments, which are consistent with the thermal analysis of the corresponding polymer networks. After solvent screening, THF was

selected as a solvent due to its compatibility with all monomers and the favorable swelling behavior observed (swelling degrees between 130% and 340%). Despite being swollen in THF, all samples were resistant to dissolution, indicating effective cross-linking and chemical bonding among the polymer chains within the network. Increasing the catalyst amount from TBD-5% to TBD-10% resulted in a decrease in the soluble fraction (from 16 to 9%), suggesting that a higher cross-link density was favored by the additional presence of TBD. The soluble fraction decreased further to 2% when the acid:epoxide ratio was reduced to 0.25:1 (Ac-25%). Additionally, this network exhibited a decrease in its swelling ratio, which may be ascribed to an increased crosslinking density and epoxy homopolymerization. The rigidity of the network structure played also an important role in altering the outcome of swelling experiments. For example, transitioning from a network of Sil-75% to one containing only DiEpoxOct (Sil-0%) resulted in a respective decrease in swelling ratio and soluble fraction from 280% and 17% to 168% and 7%, respectively. All these findings highlight the significance of regulating the reactant contents and nature to achieve the desired network properties.

Viscoelastic characterization

To investigate the dynamic behavior of vitrimers containing dual dynamic groups, reported in Table 1 and Table S1 (ESI), stress-relaxation experiments of single and dual dynamic vitrimers were carried out across a wide temperature range of 150-200 °C (Figure S23-S27, ESI). An initial basic calculation of the characteristic material stress relaxation time (τ^*) was based on the time required for the initial stress or modulus to relax to 1/e of its value. The results revealed that the dual dynamic network (TBD-10%) demonstrated dramatically shorter relaxation times in comparison to the reference vitrimers (Sil-0% and Am-3, containing the same amount of catalyst). At 200 °C, for example, the characteristic stress relaxation time of the dual dynamic

vitrimer was around 225 times faster than that of the "only siloxane-based" vitrimer (Am-3) and about 24 times faster than that of the "only ester-based" vitrimer (Sil-0%) (Figure S28, ESI). This suggests that the siloxane and ester dynamic bonds, catalyzed by TBD, work together in a synergistic manner to facilitate topology rearrangement, in an extent that is greater than what would be expected from the separate dynamic exchange chemistries.

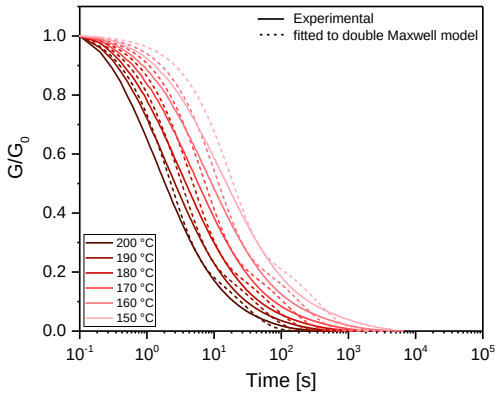

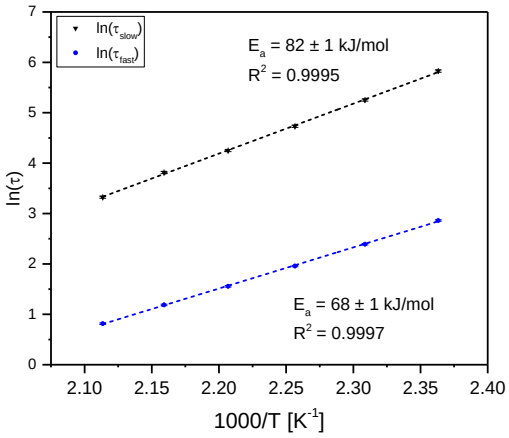

Figure 3. Normalized stress-relaxation curves of TBD-10%, fitted to the double Maxwell model (a) and Arrhenius plots generated from the deconvoluted relaxation times of both modes (b), revealing an apparent activation energy of 82 ± 1 kJ/mol and 68 ± 1 kJ/mol for the fast and slow relaxation modes, respectively.

Because of the presence of two types of dynamic bonds, the stress-relaxation data were subsequently analyzed via fitting with different models of exponential decay, namely, single Maxwell model, stretched Maxwell model and double Maxwell model. While the single Maxwell model did not provide a good fit for the stress-relaxation data of the benchmark siloxane and ester networks, the stretched Maxwell model, on the other hand, could be successfully applied (Figure S29 and Table S2, ESI). However, in the case of polymer networks containing siloxane-ester dual dynamic chemistries (TBD-10%), the best fit was only obtained using the double Maxwell model (Figure 3 and Table S3, ESI), which enables to take the two different prominent modes of stress-relaxation into account. This observation provided a first experimental support of the dual-dynamic relaxation behavior of the herein described vitrimers.

The deconvolution experiments of both segments shed light on the underlying mechanisms governing the observed stress-relaxation behavior and highlight the efficacy of the dual dynamic bonding approach in designing vitrimer materials with enhanced dynamic properties. Specifically, deconvolution allowed to virtually separate the relaxation rate of the faster from the slower relaxing segments, which were attributed to transesterification (E_a = 82 ± 1 kJ/mol) and siloxane exchange (E_a = 68 ± 1 kJ/mol), respectively (Figure 3b). Here, it was rationalized that an already relaxed ester portion located in close proximity in space to a siloxane bond, will considerably impact the relaxation rate of the dynamic siloxane bond. In particular, as previously demonstrated for the relaxation behavior of blends of linear and star-shaped polymers,[61] a neighboring relaxed fraction will act as a “solvent” because it significantly promotes diffusion. Higher temperatures resulted in faster relaxation rates and a more pronounced “solvent” effect of the faster segments in dual-dynamic vitrimers.

The dynamic properties were controlled by adjusting the network composition and the amount of catalyst used. The data indicated that the stress-relaxation of the siloxane-ester system with 10 mol% TBD occurred about three times faster than the system with 5 mol% TBD (with characteristic relaxation times τ^* of 3.3 s and 9.6 s, respectively, Fig. 4a). This is consistent with the "only siloxane-based" networks (Am-1, Am-2, and Am-3), which displayed a similar pattern, where the material containing 10 mol% TBD had a 2.5 times faster stress relaxation than the material with 5 mol% TBD (with relaxation times of $\tau^* = 748$ s and $\tau^* = 1885$ s, respectively) (Figure S30). These observations showed that higher catalyst loading could result in a larger fraction of dynamic bonds (at a specific temperature) and therefore more efficient stress-relaxation.

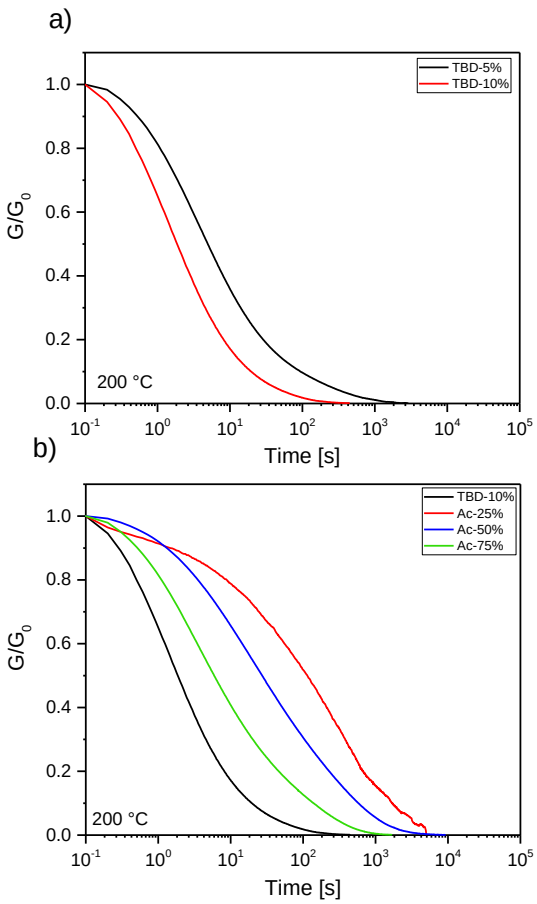

Figure 4. Comparison of stress-relaxation times at 200 °C under varying catalyst loading (a) and acid content (b).

The relaxation behavior was also strongly influenced by the acid content. Vitrimers prepared with a lower acid content exhibited slower relaxation behavior (Figure 4b). This observation is consistent with the "solvent" effect of the faster segments discussed earlier. For instance, the relaxation time of TBD-10% was found to be around 60 times faster than that of Ac-25% (τ^* = 3.3 s vs τ^* = 203 s). Additionally, with a constant acid content in the vitrimers, the siloxane content in the epoxy reactant emerged as an important factor influencing the relaxation rate, as demonstrated in Figure 5. Specifically, as the siloxane content increased, the relaxation time decreased accordingly, with the relaxation time of Sil-75%% being 6 times faster than that of Sil-0% (τ^* = 14 s and τ^* = 79 s, respectively). Sil-25% sample exhibited a distinct behavior with multiple relaxation profiles during the stress relaxation analysis (Figure 5). This can be attributed to the relatively low siloxane content in Sil-25%, which plays a pivotal role for the reprocessability. Unlike Sil-0% (no siloxane groups), and Sil-50%, Sil-75% and TBD-10%, which have higher siloxane content, this difference in composition likely contributed to the observed variability in relaxation rates across different time periods of Sil-25%.

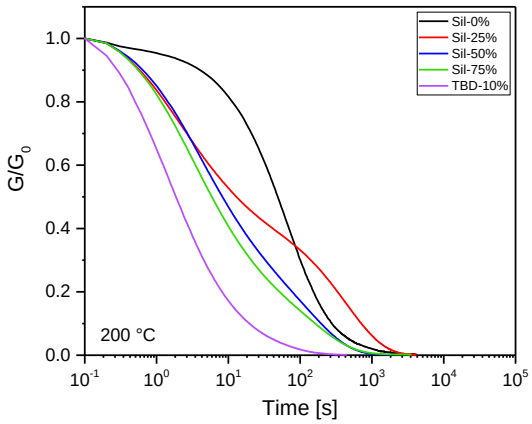

Figure 5. Comparison of stress-relaxation times with varying siloxane content.

To evaluate the endurance of the fast characteristic relaxation time of TBD-catalyzed materials through multiple mechanical recycling steps, the TBD-10% material was subjected four times to compression molding at 160 °C. After each step, the resulting sample was analyzed using FTIR, DSC, and TGA (Figure S6, S13 and S17, respectively). After undergoing recycling, the materials exhibited a slight enhancement in thermal stability, as evidenced by a marginal increase in the onset temperature of degradation ($T_{d50\%}$) from 405°C in the initial sample to 410°C in the recycled samples (R1-R4), ascribed to further crosslinking during the hot pressing process. Additionally, a stress-relaxation experiment was performed for the 4th cycle (Figure S31). The average characteristic stress relaxation times of the materials are similar (between 3 and 6 seconds). The FTIR spectra, T_g and $T_{d5\%}$ values also exhibited a remarkable similarity. These data confirm the effectiveness of TBD as a catalyst, even after multiple reprocessing cycles.

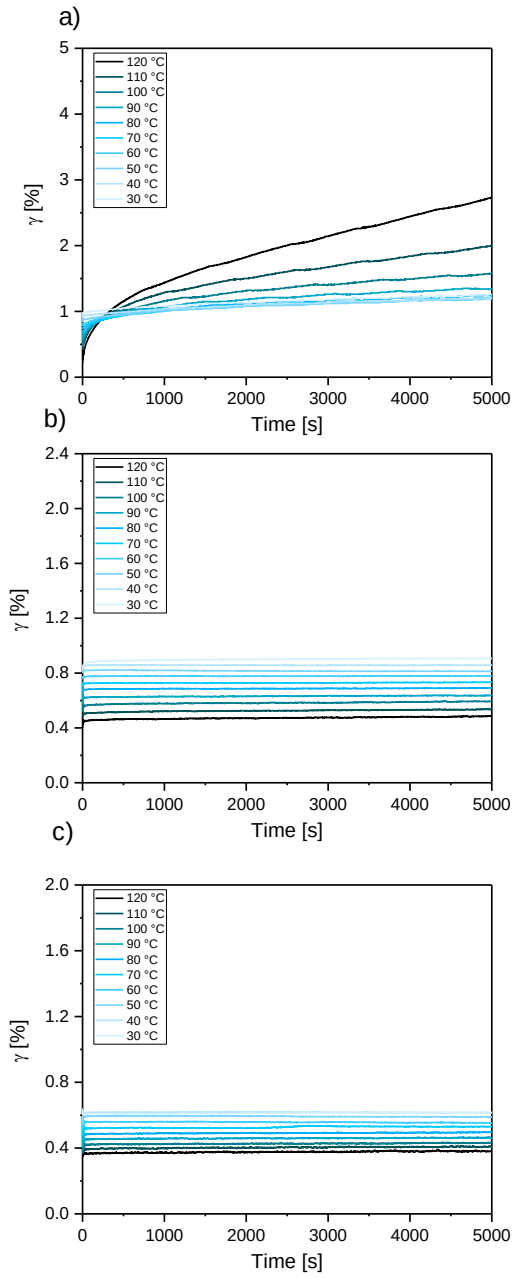

Figure 6. Creep curves (shear strain as a function of time) of respectively TBD-10% (a), Sil-0% (b) and Am-3 (c) between 30 and 120 °C with an applied shear stress σ of 2 kPa for 5000 seconds.

It is important to determine the dynamic behavior both at a short and a longer timescale to determine mechanical integrity as a function of time and temperature.[11] To that end, creep experiments were conducted for TBD-10%, Sil-0%, and Am-3%. Specifically, a constant shear

stress of 2 kPa was applied for 5000 seconds between 30 °C and 120 °C, and the resulting strain was measured over time (Figure 6). To practically verify whether the steady-state regime was reached within the measured time-intervals, the creep compliance, J(t), was plotted as a function of time.[12,62] In case of terminal relaxation (or steady-state flow), J(t) should exhibit a time scaling of 1. However, in none of the tested materials such power law scaling could be achieved, leaving out the possibility to derive meaningful creep rate (Figure S32, ESI).[63] The recorded data further indicated that the single-component systems exhibited the highest creep resistance, displaying purely instantaneous elastic deformation in which the creep compliance is dominated by entropic elasticity effects (similar to thermoset materials).[9] In the case of the dual system (TBD-10%), which showed the fastest stress-relaxation response, a higher creep sensitivity was found. This material displayed early primary creep effects while reaching a power law scaling of 0.41 at 120 °C after 5000 s. These results highlight the synergistic effect of the two dynamic bonds in the dual dynamic vitrimers, which not only resulted in faster stress relaxation but also did not necessarily lead to a much faster creep response.

CONCLUSION

This study explored the synergistic impact of incorporating siloxane and ester dynamic bonds, both catalyzed with TBD, into epoxy-acid cured vitrimers. The preparation of a series of polyhydroxy ester networks containing siloxane moieties was achieved by adjusting the concentration of (dynamic) bonds and catalyst loading. The resulting network structure was found to be greatly influenced by the acid content used in the material fabrication process, with lower acid content leading to a predominantly polyether-based network. These results demonstrated that controlling dynamic bond concentration and catalysts in vitrimer materials can effectively regulate the rate of chemical exchange reactions and enhance thermal and mechanical

properties. In addition, the dual dynamic networks displayed faster relaxation times than vitrimers containing siloxane and ester groups individually, enabling faster topology rearrangement.

ASSOCIATED CONTENT

Supporting Information. Containing Table S1 comprising the physical properties of Am-1, Am-2 and Am-3, pictures of typical reprocessed materials, FTIR spectra, ^{1}H NMR of the model reaction, DSC, TGA, stress-relaxation experiments and creep measurements.

AUTHOR INFORMATION

Corresponding Author

* Sami Fadlallah: sami.fadlallah@agroparistech.fr

* Filip E. Du Prez: filip.duprez@ugent.be

Author Contributions

All authors have given their approval to the final version of the manuscript.

Notes

The authors declare no competing financial interest.

ACKNOWLEDGMENT

The authors would like to acknowledge Grand Est region, Département de la Marne and Grand Reims for their financial support. They would also like to thank Bernhard De Meyer for technical support. This project received funding from the European Research Council (ERC) under the

European Union's Horizon 2020 research and innovation programme 101021081 (ERC-AdG-2020, CiMaC-project).

REFERENCES

[1] W. Schönthaler, Thermosets, in: Ullmann's Encyclopedia of Industrial Chemistry, Wiley-VCH Verlag GmbH & Co. KGaA, Weinheim, Germany, 2000. https://doi.org/10.1002/14356007.a26_665.

[2] E. Morici, N.T. Dintcheva, Recycling of Thermoset Materials and Thermoset-Based Composites: Challenge and Opportunity, Polymers 14 (2022) 4153. https://doi.org/10.3390/polym14194153.

[3] C.J. Kloxin, C.N. Bowman, Covalent adaptable networks: smart, reconfigurable and responsive network systems, Chemical Society Reviews 42 (2013) 7161–7173. https://doi.org/10.1039/C3CS60046G.

[4] C.N. Bowman, C.J. Kloxin, Covalent Adaptable Networks: Reversible Bond Structures Incorporated in Polymer Networks, Angewandte Chemie International Edition 51 (2012) 4272–4274. https://doi.org/10.1002/anie.201200708.

[5] C.J. Kloxin, T.F. Scott, B.J. Adzima, C.N. Bowman, Covalent Adaptable Networks (CANs): A Unique Paradigm in Cross-Linked Polymers, Macromolecules 43 (2010) 2643–2653. https://doi.org/10.1021/ma902596s.

[6] N. Zheng, Y. Xu, Q. Zhao, T. Xie, Dynamic Covalent Polymer Networks: A Molecular Platform for Designing Functions beyond Chemical Recycling and Self-Healing, Chemical Reviews 121 (2021) 1716–1745. https://doi.org/10.1021/acs.chemrev.0c00938.

[7] P. Chakma, D. Konkolewicz, Dynamic Covalent Bonds in Polymeric Materials, Angewandte Chemie International Edition 58 (2019) 9682–9695. https://doi.org/10.1002/anie.201813525.

[8] D. Montarnal, M. Capelot, F. Tournilhac, L. Leibler, Silica-Like Malleable Materials from Permanent Organic Networks, Science 334 (2011) 965–968. https://doi.org/10.1126/science.1212648.

[9] J. Luo, Z. Demchuk, X. Zhao, T. Saito, M. Tian, A.P. Sokolov, P.F. Cao, Elastic vitrimers: Beyond thermoplastic and thermoset elastomers, Matter 5 (2022) 1391–1422. https://doi.org/10.1016/J.MATT.2022.04.007.

[10] L. Porath, B. Soman, B.B. Jing, C.M. Evans, Vitrimers: Using Dynamic Associative Bonds to Control Viscoelasticity, Assembly, and Functionality in Polymer Networks, ACS Macro Letters (2022) 475–483. https://doi.org/10.1021/acsmacrolett.2c00038.

[11] F. Van Lijsebetten, T. Debsharma, J.M. Winne, F.E. Du Prez, A Highly Dynamic Covalent Polymer Network without Creep: Mission Impossible?, Angewandte Chemie International Edition 61 (2022) e2022104. https://doi.org/10.1002/anie.202210405.

[12] F. Van Lijsebetten, K. De Bruycker, Y. Spiesschaert, J.M. Winne, F.E. Du Prez, Suppressing Creep and Promoting Fast Reprocessing of Vitrimers with Reversibly Trapped Amines, Angewandte Chemie International Edition 61 (2022) e2021138. https://doi.org/10.1002/anie.202113872.

[13] S. Ciarella, F. Sciortino, W.G. Ellenbroek, Dynamics of Vitrimers: Defects as a Highway to Stress Relaxation, Physical Review Letters 121 (2018) 058003. https://doi.org/10.1103/PhysRevLett.121.058003.

[14] F. Van Lijsebetten, J.O. Holloway, J.M. Winne, F.E. Du Prez, Internal catalysis for dynamic covalent chemistry applications and polymer science, Chemical Society Reviews 49 (2020) 8425–8438. https://doi.org/10.1039/D0CS00452A.
[15] F. Cuminet, S. Caillol, É. Dantras, É. Leclerc, V. Ladmiral, Neighboring Group Participation and Internal Catalysis Effects on Exchangeable Covalent Bonds: Application to the Thriving Field of Vitrimer Chemistry, Macromolecules 54 (2021) 3927–3961. https://doi.org/10.1021/acs.macromol.0c02706.
[16] M. Capelot, M.M. Unterlass, F. Tournilhac, L. Leibler, Catalytic Control of the Vitrimer Glass Transition, ACS Macro Letters 1 (2012) 789–792. https://doi.org/10.1021/mz300239f.
[17] Y. Nishimura, J. Chung, H. Muradyan, Z. Guan, Silyl Ether as a Robust and Thermally Stable Dynamic Covalent Motif for Malleable Polymer Design, Journal of the American Chemical Society 139 (2017) 14881–14884. https://doi.org/10.1021/jacs.7b08826.
[18] O.R. Cromwell, J. Chung, Z. Guan, Malleable and Self-Healing Covalent Polymer Networks through Tunable Dynamic Boronic Ester Bonds, Journal of the American Chemical Society 137 (2015) 6492–6495. https://doi.org/10.1021/jacs.5b03551.
[19] D.N. Barsoum, V.C. Kirinda, B. Kang, J.A. Kalow, Remote-Controlled Exchange Rates by Photoswitchable Internal Catalysis of Dynamic Covalent Bonds, Journal of the American Chemical Society 144 (2022) 10168–10173. https://doi.org/10.1021/JACS.2C04658/ASSET/IMAGES/LARGE/JA2C04658_0003.JPEG .
[20] T. Debsharma, V. Amfilochiou, A.A. Wróblewska, I. De Baere, W. Van Paepegem, F.E. Du Prez, Fast Dynamic Siloxane Exchange Mechanism for Reshapable Vitrimer Composites, Journal of the American Chemical Society 144 (2022) 12280–12289. https://doi.org/10.1021/jacs.2c03518.
[21] V. Zhang, B. Kang, J. V. Accardo, J.A. Kalow, Structure–Reactivity–Property Relationships in Covalent Adaptable Networks, Journal of the American Chemical Society (2022). https://doi.org/10.1021/JACS.2C08104.
[22] G.M. Scheutz, J.J. Lessard, M.B. Sims, B.S. Sumerlin, Adaptable Crosslinks in Polymeric Materials: Resolving the Intersection of Thermoplastics and Thermosets, J. Am. Chem. Soc. 141 (2019) 16181–16196. https://doi.org/10.1021/jacs.9b07922.
[23] N. Zee, R. Nicolay, Vitrimers: Permanently crosslinked polymers with dynamic network topology, Progress in Polymer Science 104 (2020) 101233. https://doi.org/10.1016/j.progpolymsci.2020.101233.
[24] W. Denissen, J.M. Winne, F.E.D. Prez, Vitrimers: permanent organic networks with glass-like fluidity, Chem. Sci. 7 (2015) 30–38. https://doi.org/10.1039/C5SC02223A.
[25] M. Capelot, D. Montarnal, F. Tournilhac, L. Leibler, Metal-catalyzed transesterification for healing and assembling of thermosets, Journal of the American Chemical Society 134 (2012) 7664–7667. https://doi.org/10.1021/ja302894k.
[26] J.P. Brutman, P.A. Delgado, M.A. Hillmyer, Polylactide Vitrimers, ACS Macro Letters 3 (2014) 607–610. https://doi.org/10.1021/mz500269w.
[27] J.L. Self, N.D. Dolinski, M.S. Zayas, J. Read de Alaniz, C.M. Bates, Brønsted-Acid-Catalyzed Exchange in Polyester Dynamic Covalent Networks, ACS Macro Letters 7 (2018) 817–821. https://doi.org/10.1021/acsmacrolett.8b00370.

[28] A. Gablier, M.O. Saed, E.M. Terentjev, Transesterification in Epoxy–Thiol Exchangeable Liquid Crystalline Elastomers, Macromolecules 53 (2020) 8642–8649. https://doi.org/10.1021/acs.macromol.0c01757.
[29] A. Gablier, M.O. Saed, E.M. Terentjev, Rates of transesterification in epoxy–thiol vitrimers, Soft Matter 16 (2020) 5195-5202. https://doi.org/10.1039/D0SM00742K.
[30] K. Tangthana-Umrung, Q.A. Poutrel, M. Gresil, Epoxy Homopolymerization as a Tool to Tune the Thermo-Mechanical Properties and Fracture Toughness of Vitrimers, Macromolecules 54 (2021) 8393–8406. https://doi.org/10.1021/ACS.MACROMOL.1C00861/ASSET/IMAGES/LARGE/MA1C00861_0014.JPEG.
[31] Q.-A. Poutrel, J.J. Blaker, C. Soutis, F. Tournilhac, M. Gresil, Dicarboxylic acid-epoxy vitrimers: influence of the off-stoichiometric acid content on cure reactions and thermo-mechanical properties, Polymer Chemistry 11 (2020) 5327–5338. https://doi.org/10.1039/D0PY00342E.
[32] S. Ne Chappuis, P. Edera, M. Cloitre, F. Ois Tournilhac, Enriching an Exchangeable Network with One of Its Components: The Key to High-Tg Epoxy Vitrimers with Accelerated Relaxation, Macromolecules 55 (2022) 6982–6991. https://doi.org/10.1021/ACS.MACROMOL.2C01005.
[33] A. Demongeot, S.J. Mougnier, S. Okada, C. Soulié-Ziakovic, F. Tournilhac, Coordination and catalysis of Zn2+ in epoxy-based vitrimers, Polymer Chemistry 7 (2016) 4486–4493. https://doi.org/10.1039/C6PY00752J.
[34] C. Taplan, M. Guerre, J.M. Winne, F.E. Du Prez, Fast processing of highly crosslinked, low-viscosity vitrimers, Materials Horizons 7 (2020) 104–110. https://doi.org/10.1039/C9MH01062A.
[35] J. Han, T. Liu, C. Hao, S. Zhang, B. Guo, J. Zhang, A Catalyst-Free Epoxy Vitrimer System Based on Multifunctional Hyperbranched Polymer, Macromolecules 51 (2018) 6789–6799. https://doi.org/10.1021/acs.macromol.8b01424.
[36] R.L. Snyder, D.J. Fortman, G.X. De Hoe, M.A. Hillmyer, W.R. Dichtel, Reprocessable Acid-Degradable Polycarbonate Vitrimers, Macromolecules 51 (2018) 389–397. https://doi.org/10.1021/acs.macromol.7b02299.
[37] M. Hayashi, R. Yano, Fair Investigation of Cross-Link Density Effects on the Bond-Exchange Properties for Trans-Esterification-Based Vitrimers with Identical Concentrations of Reactive Groups, Macromolecules 53 (2020) 182–189. https://doi.org/10.1021/acs.macromol.9b01896.
[38] A. Breuillac, A. Kassalias, R. Nicolaÿ, Polybutadiene Vitrimers Based on Dioxaborolane Chemistry and Dual Networks with Static and Dynamic Cross-links, Macromolecules 52 (2019) 7102–7113. https://doi.org/10.1021/acs.macromol.9b01288.
[39] F. Van Lijsebetten, K. De Bruycker, J.M. Winne, F.E. Du Prez, Masked Primary Amines for a Controlled Plastic Flow of Vitrimers, ACS Macro Letters 11 (2022) 919–924. https://doi.org/10.1021/acsmacrolett.2c00255.
[40] L. Li, X. Chen, K. Jin, J.M. Torkelson, Vitrimers Designed Both To Strongly Suppress Creep and To Recover Original Cross-Link Density after Reprocessing: Quantitative Theory and Experiments, Macromolecules 51 (2018) 5537–5546. https://doi.org/10.1021/acs.macromol.8b00922.

[41] J.J. Cash, T. Kubo, D.J. Dobbins, B.S. Sumerlin, Maximizing the symbiosis of static and dynamic bonds in self-healing boronic ester networks, Polymer Chemistry 9 (2018) 2011–2020. https://doi.org/10.1039/C8PY00123E.
[42] Z. Song, Z. Wang, S. Cai, Mechanics of vitrimer with hybrid networks, Mechanics of Materials 153 (2021) 103687. https://doi.org/10.1016/j.mechmat.2020.103687.
[43] T. Stukenbroeker, W. Wang, J.M. Winne, F.E. Du Prez, R. Nicolaÿ, L. Leibler, Polydimethylsiloxane quenchable vitrimers, Polymer Chemistry 8 (2017) 6590–6593. https://doi.org/10.1039/C7PY01488K.
[44] B. Soman, C.M. Evans, Effect of precise linker length, bond density, and broad temperature window on the rheological properties of ethylene vitrimers, Soft Matter 17 (2021) 3569–3577. https://doi.org/10.1039/D0SM01544J.
[45] C. Taplan, M. Guerre, F.E. Du Prez, Covalent Adaptable Networks Using β-Amino Esters as Thermally Reversible Building Blocks, Journal of the American Chemical Society 143 (2021) 9140–9150. https://doi.org/10.1021/jacs.1c03316.
[46] B. Zhang, J. Ke, J.R. Vakil, S.C. Cummings, Z.A. Digby, J.L. Sparks, Z. Ye, M.B. Zanjani, D. Konkolewicz, Dual-dynamic interpenetrated networks tuned through macromolecular architecture, Polymer Chemistry 10 (2019) 6290–6304. https://doi.org/10.1039/c9py01387c.
[47] H. Wang, Y. Huang, S. V Wanasinghe, N. De, A. Watuthanthrige, D. Konkolewicz, Interpenetrated Triple Network Polymers: Synergies of Three Different Dynamic Bonds, Polymer Chemistry 8 (2022) 5255–5446. https://doi.org/10.1039/D2PY00575A.
[48] E.M. Foster, E.E. Lensmeyer, B. Zhang, P. Chakma, J.A. Flum, J.J. Via, J.L. Sparks, D. Konkolewicz, Effect of Polymer Network Architecture, Enhancing Soft Materials Using Orthogonal Dynamic Bonds in an Interpenetrating Network, ACS Macro Letters 6 (2017) 495–499. https://doi.org/10.1021/ACSMACROLETT.7B00172/SUPPL_FILE/MZ7B00172_SI_001.PDF.
[49] Y. Yang, Q. Song, C. Li, J. Tan, Y. Xue, Z. Su, G. Zhang, Q. Zhang, Reprocessable epoxy resins based on hydroxy-thioester and thiol-thioester dual exchanges, Industrial & Engineering Chemistry Research 59 (2020) 4936–4944. https://doi.org/10.1021/acs.iecr.9b06520.
[50] M. Chen, L. Zhou, Y. Wu, X. Zhao, Y. Zhang, Rapid Stress Relaxation and Moderate Temperature of Malleability Enabled by the Synergy of Disulfide Metathesis and Carboxylate Transesterification in Epoxy Vitrimers, ACS Macro Letters 8 (2019) 255–260. https://doi.org/10.1021/acsmacrolett.9b00015.
[51] J.R. Vakil, N. De Alwis Watuthanthrige, Z.A. Digby, B. Zhang, H.A. Lacy, J.L. Sparks, D. Konkolewicz, Controlling polymer architecture to design dynamic network materials with multiple dynamic linkers, Molecular Systems Design & Engineering 5 (2020) 1267–1276. https://doi.org/10.1039/D0ME00015A.
[52] D.J. Fortman, R.L. Snyder, D.T. Sheppard, W.R. Dichtel, Rapidly Reprocessable Cross-Linked Polyhydroxyurethanes Based on Disulfide Exchange, ACS Macro Letters 7 (2018) 1226–1231. https://doi.org/10.1021/ACSMACROLETT.8B00667/SUPPL_FILE/MZ8B00667_SI_001.PDF.

[53] O.J. Dodo, L. Petit, D. Dunn, C.P. Myers, D. Konkolewicz, Thermoresponsive, Recyclable, Conductive, and Healable Polymer Nanocomposites with Three Distinct Dynamic Bonds, ACS Appl. Polym. Mater. 4 (2022) 6850–6862. https://doi.org/10.1021/acsapm.2c00790.
[54] G. Lee, H.Y. Song, S. Choi, C. Bin Kim, K. Hyun, S.-K. Ahn, Harnessing β-Hydroxyl Groups in Poly(β-Amino Esters) toward Robust and Fast Reprocessing Covalent Adaptable Networks, Macromolecules 55 (2022) 10366–10376. https://doi.org/10.1021/acs.macromol.2c01872.
[55] Dimitri Berne, Guilhem Coste, Roberto Morales-Cerrada, Marine Boursier, Julien Pinaud, Vincent Ladmiral, Sylvain Caillol, Taking advantage of β-hydroxy amine enhanced reactivity and functionality for the synthesis of dual covalent adaptable networks, Polymer Chemistry 13 (2022) 3806–3814. https://doi.org/10.1039/D2PY00274D.
[56] Y. Sun, M. Wang, Z. Wang, Y. Mao, L. Jin, K. Zhang, Y. Xia, H. Gao, Amine-Cured Glycidyl Esters as Dual Dynamic Epoxy Vitrimers, Macromolecules 55 (2022) 523–534. acs.macromol.1c01914. https://doi.org/10.1021/ACS.MACROMOL.1C01914.
[57] L. Porath, J. Huang, N. Ramlawi, M. Derkaloustian, R.H. Ewoldt, C.M. Evans, Relaxation of Vitrimers with Kinetically Distinct Mixed Dynamic Bonds, Macromolecules 55 (2022) 4450–4458. https://doi.org/10.1021/acs.macromol.1c02613.
[58] B. Rupasinghe, J.C. Furgal, Degradation of silicone-based materials as a driving force for recyclability, Polymer International 71 (2022) 521–531. https://doi.org/10.1002/pi.6340.
[59] F. Van Lijsebetten, K. De Bruycker, E. Van Ruymbeke, J.M. Winne, F.E. Du Prez, Characterising different molecular landscapes in dynamic covalent networks, Chemical Science 13 (2022) 12865–12875. https://doi.org/10.1039/D2SC05528G.
[60] M. Hayashi, Dominant Factor of Bond-Exchange Rate for Catalyst-Free Polyester Vitrimers with Internal Tertiary Amine Moieties, ACS Appl. Polym. Mater. 2 (2020) 5365–5370. https://doi.org/10.1021/acsapm.0c01099.
[61] M.E. Shivokhin, E. van Ruymbeke, C. Bailly, D. Kouloumasis, N. Hadjichristidis, A.E. Likhtman, Understanding Constraint Release in Star/Linear Polymer Blends, Macromolecules 47 (2014) 2451–2463. https://doi.org/10.1021/ma402475a.
[62] R.G. Ricarte, F. Tournilhac, M. Cloître, L. Leibler, Linear Viscoelasticity and Flow of Self-Assembled Vitrimers: The Case of a Polyethylene/Dioxaborolane System, Macromolecules 53 (2020) 1852–1866. https://doi.org/10.1021/acs.macromol.9b02415.
[63] V. Scholiers, B. Hendriks, S. Maes, T. Debsharma, J.M. Winne, F.E. Du Prez, Trialkylsulfonium-Based Reprocessable Polyurethane Thermosets, Macromolecules 56 (2023) 9559–9569. https://doi.org/10.1021/acs.macromol.3c01270.